جمهورية العراق
وزارة التعليم العالي والبحث العلمي
جامعة الانبار
كلية التربية للبنات
قسم الكيمياء

Molecular Docking Study of Biphenyl-2-Oxadiazole Analogues as COX-2 Inhibitors

دراسة الارساء الجزيئي لنظائر مركب (Biphenyl-2-Oxadiazole) كمثبط لانزيم (COX2)

مشروع بحث تخرج مقدم الى رئاسة قسم الكيمياء / كلية التربية بنات/جامعة الانبار
كجزء من متطلبات نيل شهادة البكلوريوس في الكيمياء

اعداد الطالبة:
صبا محمد كسار

اشراف
د. محمد عدي

March, 2017

الاهداء

اهدي هذا العمل الى:

القلب الكبير (والدي العزيز)

القلب الناصع البياض (والدتي الحبيبة)

القلب الكبير (والدي العزيز)
القلب الناصع البياض (والدتي الحبيبة)

شكر وتقدير

اتقدم بالشكر الجزيل الى الاستاذ المشرف د. محمد عدي على ما قام به من متابعة علمية للاشراف على البحث و الى كل من ساهم وساعد على انجاز هذا العمل.

قائمة المحتويات

Abstract

This research has been carried out on (Molecular Docking of VMSB-based Compounds for COX2 Enzyme Inhibition: Simulation Study). The study has been included molecular docking simulation to evaluate the effect of VMSB compounds on the inhibition of inflammation. Results of the virtual docking process have showed that the top three VMSB compounds in terms of energy score were VMSB2, VMSB12, and VMSB6. These compounds have energy score of -10. 067, -10. 029, and -9. 922 respectively.

CHAPTER ONE
INTRODUCTION

Drug industry has been increased recently due to the discovery of new techniques that help in developing this industry. Structure-based drug design (SBDD) methods are a prominent component of modern medicinal chemistry [1]. In addition to pharmacodynamics data (e.g., potency, affinity, efficacy, selectivity), pharmacokinetic properties (ADMET: absorption, distribution, metabolism, excretion and toxicity) have also been studied through the application of these methodologies [2]. The field has progressed hand-in-hand with advances in biomolecular spectroscopic methods such as X-ray crystallography and nuclear magnetic resonance (NMR), which have enabled striking progress in molecular and structural biology. These techniques have allowed the resolution of more than 100,000 three-dimensional protein structures, providing vital structural information about key macromolecular drug targets [3].

Molecular docking is one of the SBDD methods used to evaluate the ligand conformation in a target binding place. Molecular docking has become one of the most important tools in drug design since its first algorithm discovery in 1980s [4]. Docking can be achieved through two interrelated steps: first by sampling conformations of the ligand in the active site of the protein; then ranking these conformations via a scoring function. Ideally, sampling algorithms should be able to reproduce the experimental binding mode and the scoring function should also rank it highest among all generated conformations [5]. Ligand is a small molecule, which interacts with protein’s binding sites. There are several possible mutual

conformations in which binding may occur [6]. Furthermore, molecular docking algorithms execute quantitative predictions of binding energetics, providing rankings of docked compounds based on the binding affinity of ligand-receptor complexes [4,7]. Figure (1) shows the outlines of the molecular docking process which states how to dock the ligand into a receptor. In this figure, part A shows a three dimensional structure for the ligand whereas part B is for the receptor. The docking of the ligand in the cavity of the receptor is shown in part C; part D explores the binding conformation and the corresponding intermolecular interactions. In this study, molecular docking will be carried out on 1,3,4-Oxadiazole compound using Autodock software. Oxadiazole compounds are intended to be docked with the cyclooxygenase enzyme (COX).

COX is the enzyme involved in the body due to the inflammation and is responsible for the formation of prostanoids which are the key part of inflammation development [8]. There are two COX isoforms, which differ mainly in their pattern of expression. Cycloxygenase-1 was first purified from bovine vesicular glands in 1976. COX-1 is constitutively expressed in many tissues including kidney, lung, stomach, duodenum, jejunum, ileum, colon, and cecum of rat, dog, Rhesus monkey, and human [9]. COX-1 activity is believed to be responsible for producing cytoprotective prostaglandins, such as prostacyclin and PGE2, which are thought to be critical to maintain integrity of gastric mucosa [10]. The second isoform is isolated in 1991, now known as cyclooxygenase-2 (COX-2), shares significant sequence homology and catalytic activity with COX-1. However, its expression pattern is markedly different. Most tissues, with the exception of the placenta, the macula densa of the kidney and brain, do not constitutively express COX-2 [11].

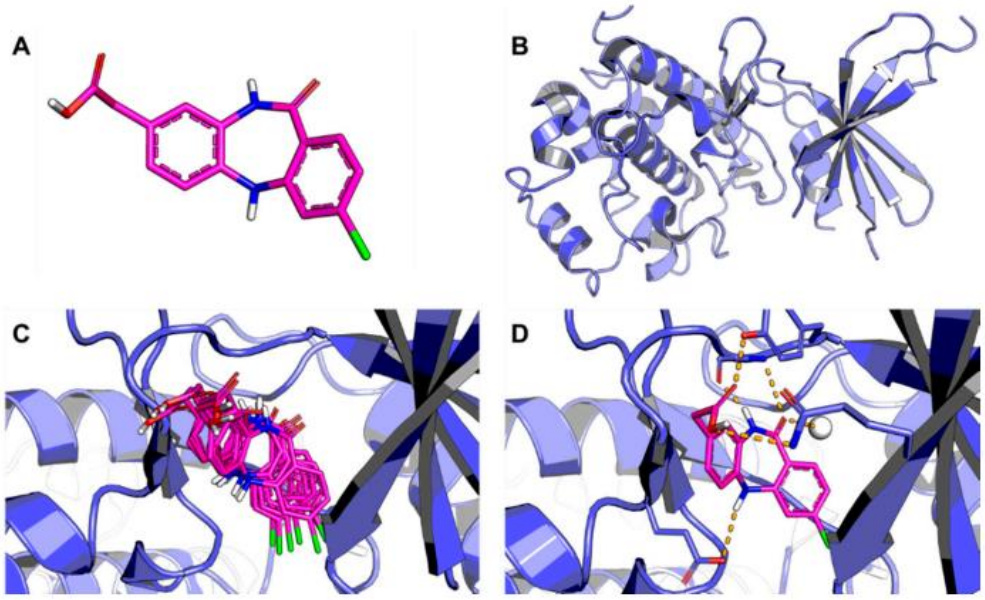

Figure 1. Molecular docking process [12]

Oxadiazole is one of the heterocyclic compounds. These compounds contains besides carbon atoms, one or more of other elements. The sequence of these atoms may be different as 1,2,4-oxadiazole (a), 1,2,5-oxadiazole (b), 1,2,3-oxadiazole (c) and 1,3,4-oxadiazol(d) [13], see Figure (2). The non-carbon atoms in such ring are adopted as hetero atoms. The common hetero atoms are nitrogen, oxygen and sulphur. The important of heterocyclic compounds are present in most of the members of vitamin B complex, antibiotics, alkaloids, amino acids, drugs, dyes, enzyme & genetic material, DNA and having therapeutics use [14]. 1,3,4-oxadiazole is a 5-membered heterocyclic compound. At room temperature it is liquid in nature and having boiling point at 150^{o}C. 1,3,4-oxadiazole have good thermal stability. It is prepared by method reported [15]. Antimicrobial activities of 1,3,4-oxadiazole derivatives like, antibacterial activity against *Staphylococcus aureus, Escherichia coli, Pseudomonas aeruginosa* and antifungal activity against *Candida albicans* were studied by Rollas et al [16] for 3-acetyl-5-(4-flourophenyl)-2-substituted-2,3-dihydro-1,3,4-oxadiazoles.

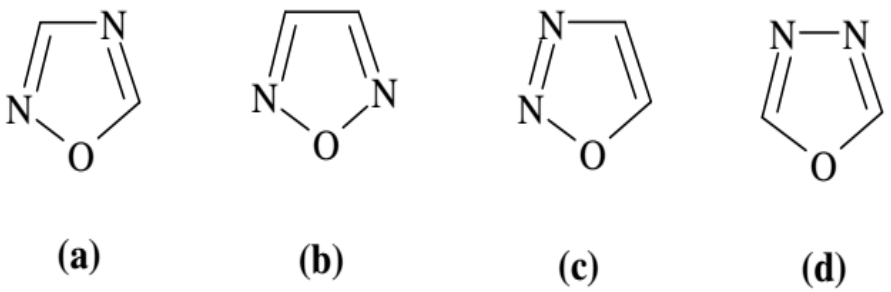

Figure 2. Different arrangement of atoms in Oxadiazole compounds.

1,3,4-Oxadiazole derivatives have many pharmaceutical applications. Some activities like anti-micropial, anti-inflamatory, analgesic, Anticonvulsant, and anti-cancer were tested using 1,3,4-Oxadiazole derivatives [17].

Many software have been used in the conduction of simulation of molecular docking. ADAM, Glide, AutoDock, AutoDock Vina, and BetaDock are some examples for these software. In this study AutoDock software will be used to study the docking process.

The objective of this work is to study numerically the optimum conformation through a docking process that will be carried out on biphenyl-2-oxadiazoles.

CHAPTER TWO
METHOD

The structures of all compounds were drawn using ChemDraw Ultra from the ChemOffice software package, as seen in figures (3-17). Then, it was copied into Chem3D Ultra (same program package), where it was subjected to simplified energy minimization search to a minimum root mean standard deviation gradient of 0.100. The chemical structures of the compounds of interest were drawn, and their geometry was optimized using MM+ force field. The obtained structure with local minimum was saved in convenient mol2 format. The enzyme downloaded from the RCSB Protein Data Bank (PDB) and the protein refined in to be use for docking process. After obtaining the ligands and enzymes, their structures were converted to pdbqt format, using the Auto Dock Tools 1.5.4 program, in which all the rotatable bonds of ligands were allowed to rotate freely, and the receptors were considered rigid. In silico docking study was perform by using Auto Dock 4.2. and docking calculation was performed using the refined protein and the desired ligand in .pdb format. The enzyme molecule is saved as Protein.pdb. Toggle the "Auto Dock" TOOLS, the ligand is from the file via input option. The torsions were analyzed and finally the ligand is saved in the Cygwin location as ligand.pdbqt. Then Auto Grid calculation performed and save it as "Protein.gpf" file. With 1 ˚A of spacing between the grid points. The grid box was centered on the active site of the enzymes with high resolution, allowing the program to search for additional places of probable interactions between the ligands and the receptor. Other configurations were considered default. AutoDock requires pre-computed grid maps, and since the free energy scoring function incorporates solvation free energies, Stouten atomic solvation parameters and fractional volumes were assigned to the atoms using AddSol, an AutoDock utility. Atomic affinity and electrostatic

potential grid maps were calculated using AutoGrid. A grid map with 50×50×50 points and a grid point spacing of 0.375 A generously included the whole binding site. All the dockings performed in this work were carried out using the Lamarckian Genetic Algorithm (LGA). The specific AutoDock parameters for the LGA were set as follows: the population size was 50 individuals, each of whose initial translations, orientations and torsions were set to random values. The limit of the number of energy evaluations was set to 1×106 for each docking. The maximum number of generations was set to 27,000. The mutation and crossover rates were set to 0.02 and 0.80 respectively. The maximum number of iterations per local search was set to 300, and the probability of performing such a local search on an individual was 0.06. The maximum number of consecutive successes or failures before doubling or halving the local search step size was 4. Elitism was applied, with the top-scoring individual in the current generation automatically surviving into the next generation. A set of 100 docking calculations was performed for each ligand, and the resulting docked conformations were clustered into families of like-conformations, using a root mean squared positional deviation cluster tolerance of 1.0 A. These same docked conformations were re-clustered at a more forgiving value of 3.0 A. Importantly, some enzymes do not present the RMSD value because they do not have inhibitor on their structures. The RMSD value (less than 2 ˚A) is a criterion often used for correcting bound structure prediction. Programming for the docking simulation is done through Cygwin interface by using commands. Once docking has completed, toggle the Auto Dock icon and see for the 10 different conformations. The docking performed here is of rigid docking which involves the confirmations of ligand only. The redockings were performed with the same configurations of the previous performed dockings.

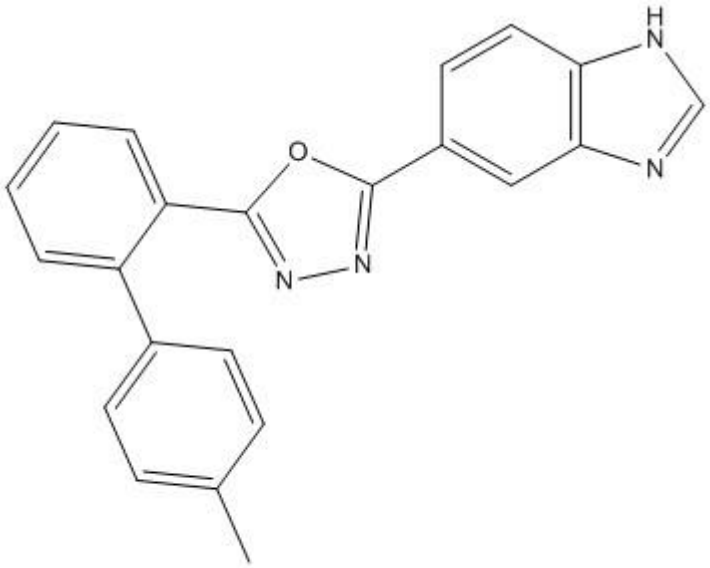

2-(1*H*-benzo[*d*]imidazol-5-yl)-5-(4'-methyl-[1,1'-biphenyl]-2-yl)-1,3,4-oxadiazole

Figure 3. Cyclic structure of VMSB1

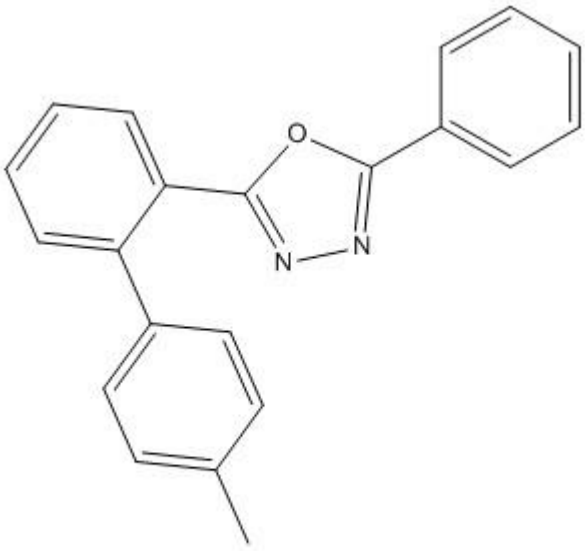

2-(4'-methyl-[1,1'-biphenyl]-2-yl)-5-phenyl-1,3,4-oxadiazole

Figure 4. Cyclic structure of VMSB2

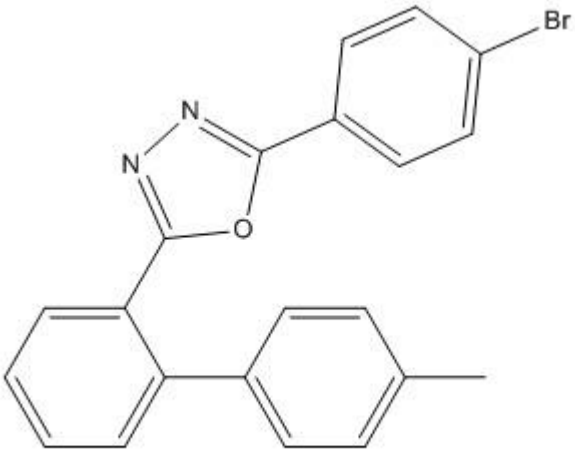

2-(4-bromophenyl)-5-(4'-methyl-[1,1'-biphenyl]-2-yl)-1,3,4-oxadiazole

Figure 5. Cyclic structure of VMSB3

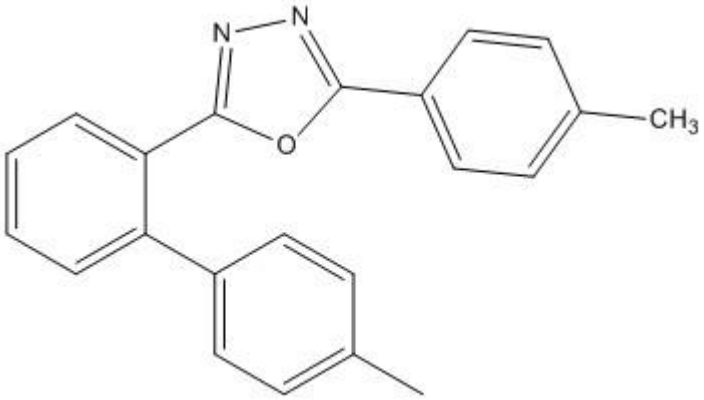

2-(4'-methyl-[1,1'-biphenyl]-2-yl)-5-(*p*-tolyl)-1,3,4-oxadiazole

Figure 6. Cyclic structure of VMSB4

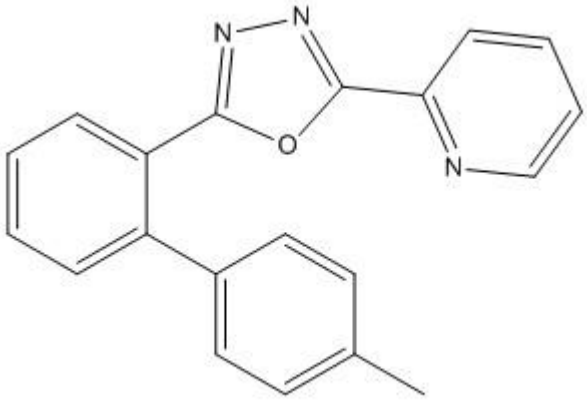

2-(4'-methyl-[1,1'-biphenyl]-2-yl)-5-(pyridin-2-yl)-1,3,4-oxadiazole

Figure 7. Cyclic structure of VMSB5

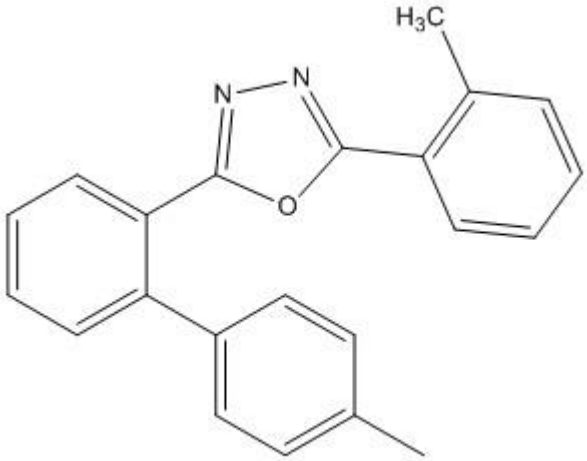

2-(4'-methyl-[1,1'-biphenyl]-2-yl)-5-(*o*-tolyl)-1,3,4-oxadiazole

Figure 8. Cyclic structure of VMSB6

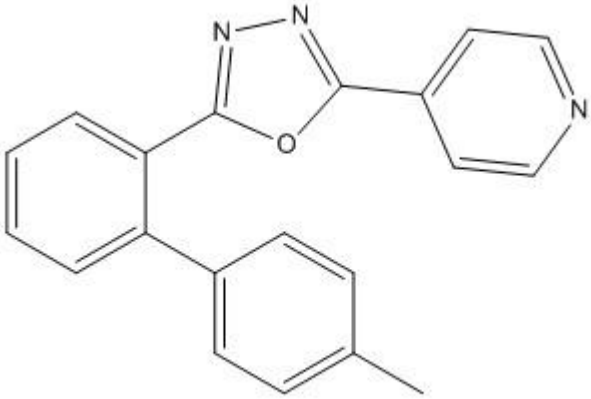

2-(4'-methyl-[1,1'-biphenyl]-2-yl)-5-(pyridin-4-yl)-1,3,4-oxadiazole

Figure 9. Cyclic structure of VMSB7

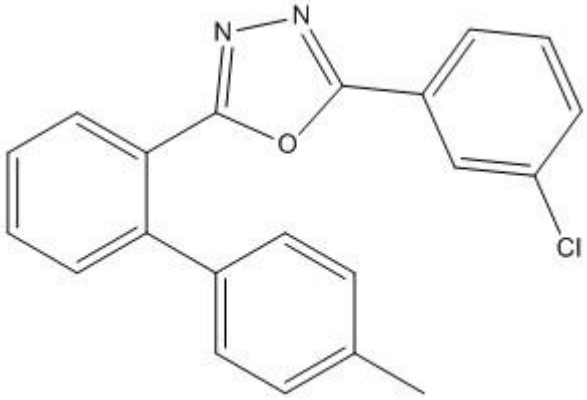

2-(3-chlorophenyl)-5-(4'-methyl-[1,1'-biphenyl]-2-yl)-1,3,4-oxadiazole

Figure 10. Cyclic structure of VMSB8

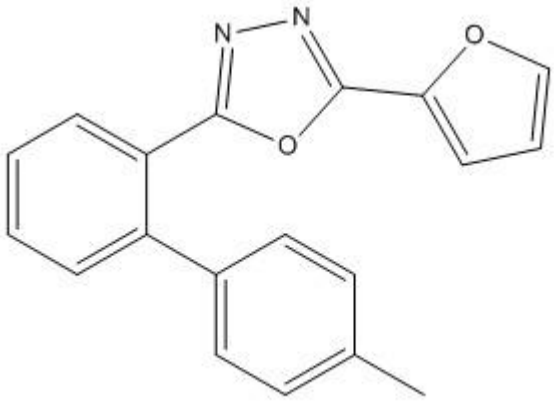

2-(furan-2-yl)-5-(4'-methyl-[1,1'-biphenyl]-2-yl)-1,3,4-oxadiazole

Figure 11. Cyclic structure of VMSB9

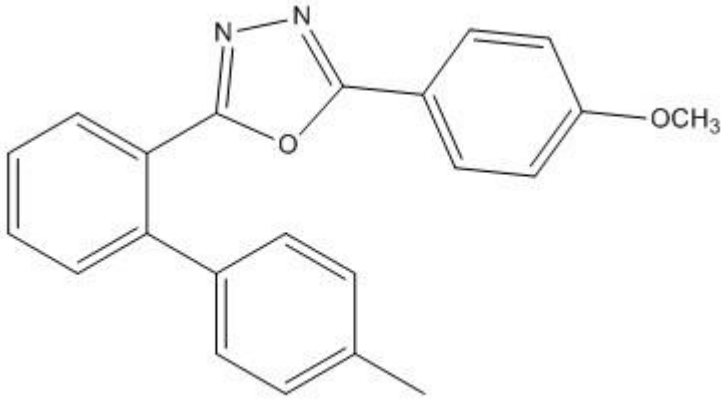

2-(4-methoxyphenyl)-5-(4'-methyl-[1,1'-biphenyl]-2-yl)-1,3,4-oxadiazole

Figure12. Cyclic structure of VMSB10

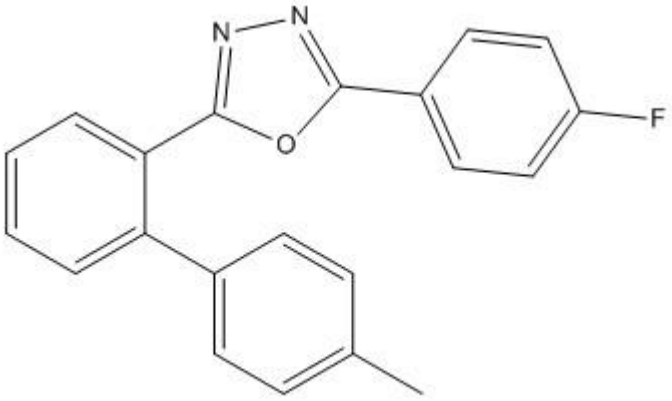

2-(4-fluorophenyl)-5-(4'-methyl-[1,1'-biphenyl]-2-yl)-1,3,4-oxadiazole

Figure 13. Cyclic structure of VMSB11

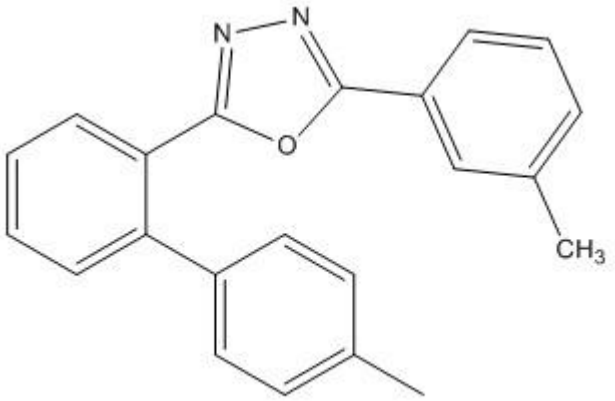

2-(4'-methyl-[1,1'-biphenyl]-2-yl)-5-(*m*-tolyl)-1,3,4-oxadiazole

Figure 14. Cyclic structure of VMSB12

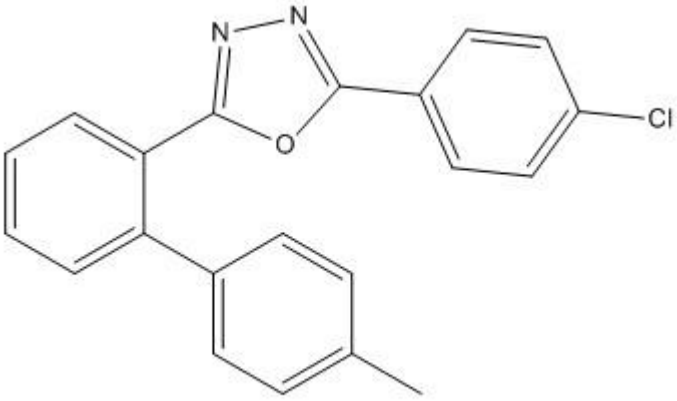

2-(4-chlorophenyl)-5-(4'-methyl-[1,1'-biphenyl]-2-yl)-1,3,4-oxadiazole

Figure 15. Cyclic structure of VMSB13

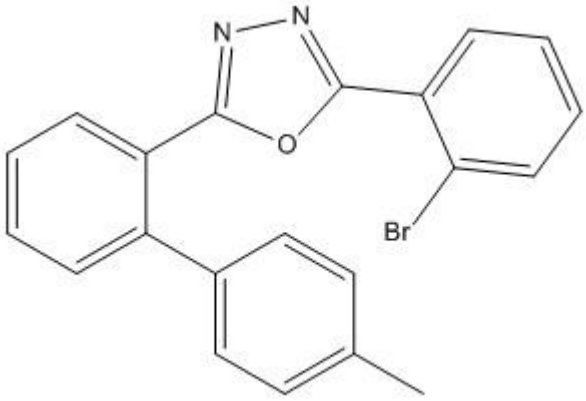

2-(2-bromophenyl)-5-(4'-methyl-[1,1'-biphenyl]-2-yl)-1,3,4-oxadiazole

Figure 16. Cyclic structure of VMSB14

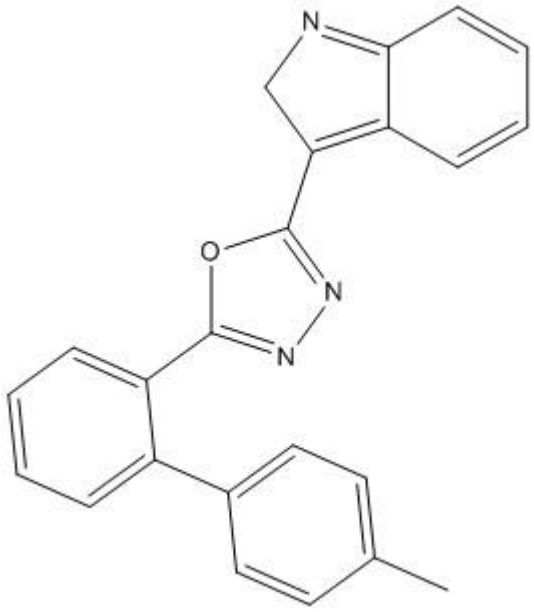

Figure 17. Cyclic structure of VMSB15

CHAPTER THREE
RESULTS AND DISCUSSION

Table (1) shows the results of docking score obtained by the docking simulation for the 15 VMSB compounds. The bonding types and the active site residues results are extracted from the images shown in figures (18-32).

According to the table below, the top three compounds are VMSB2, VMSB12, and VMSB6. These three compounds are linked to the amino acid TPR373 which is thought to be the main cause beyond the increment of the values of the docking score. The values of these three compounds are -10.067, -10.029, and -9.922 respectively. The last three compounds in the list are VMSB15, VMSB5, and VMSB13, respectively. In spite of this result, it was noted that VMSB5 is linked to the amino acid TRP373. This could be attributed to the presence of nitrogen molecule in the active site of the compound.

VMSB11 and VMSB14 have close values of docking score. Both compounds are linked to the amino acid TRP373 but contain a bond with the elements F and Br which reduce the docking score and this can be the reason for the current rank of these two compounds. Knowing that the element F reduce the energy of the active site more than the element Br, therefore the rank of VMSB14 which contain Br-Bond is higher than VMSB11 which contains F-bond.

Table (1) Docking score for the fifteen VMSB-based compounds

Compound	Docking Score (binding affinity)	Interactions	Active site Residues within 4 °A
VMSB2	-10. 067	Pi-Pi Stacking (TRP 373), Pi-cation (ARG 106)	GLY512, TYR371, TRP373, SER516,ALA513,VAL335, ARG106, LEU517, MET99, VAL102, TYR341, LEU345, SER339, LEU338, VAL509, HIE75, PHE504, ARG499, ILE503, GLN178, MET508, LEU370, PHE367
VMSB12	-10. 029	Pi-Pi Stacking (TRP 373), Pi-Pi Stacking (TYR 341), Pi-cation (ARG 106)	TYR371, LEU370, VAL335, TRP373, TYR341, SER516, ARG106, ALA513, VAL102, LEU517,MET99, LEU345, SER339, LEU338, VAL509, HIE75, ARG499,PHE504, ILE503, GLN178, GLY512, MET508, PHE367
VMSB6	-9. 922	Pi-Pi Stacking (TRP 373), Pi-cation (ARG 106), Pi-Pi Stacking (TYR 341)	GLE512, TYR371, TRP373, SER516, ALA513, VAL335, ARG106, LEU517, MET99, VAL102, LEU345, TYR341, SER339, HIE75, ILE503, ARG499, PHE504, LEU338, GLN178, VAL509, MET508, LEU370, PHE367
VMSB14	-9. 705	Pi-Pi Stacking (TRP 373), Pi-cation (ARG 106), Pi-Pi Stacking (ARG 106)	GLE512, PHE367, TYR371, VAL335, TRP373, SER516, ARG106, ALA513, LEU517, MET99, VAL102, LEU345, TYR341, SER339, VAL09, HIE75, ILE503, ARG499, PHE504, LEU338, GLN178, MET508, LEU370
VMSB11	-9. 683	Pi-Pi Stacking (TRP 373), Pi-Pi Stacking (ARG 106)), Pi-cation (ARG 106)	GLE512,TYR371, TRP373, SER516, ALA513, VAL335, ARG106, LEU517, MET99, VAL102, LEU345, TYR341, SER339, VAL509, HIE75, ARG499, ILE503, PHE504, LEU338, GLN178, MET508, LEU370, PHE367

VMSB7	-9. 462	Pi-Pi Stacking (TRP 373), Pi-Pi Stacking (ARG 106), Pi-Pi Stacking (TYR 341)	VAL102, MET99, LEU517, ARG106, TYR341, VAL535, SER516, ALA513, TRP373, TYR371, PHE367, LEU370, GL512, MET508, LEU338, VAL509, PHE504, SER339, HIE75, LEU345,
VMSB9	-9. 35	Pi-Pi Stacking (TRP 373), Pi-cation (ARG 106)	PHE367, TRP373, SER516, GLY512, VAL335, ARG106, LAL513, LEU517, TYR341, VAL102, LEU345, SER339, LEU338, VAL509, HIE75, ILE503, ARG499, PHE504, ALA502, GLN178, MET508, TYR371, LEU370
VMSB4	-8. 573	Pi-Pi Stacking (ARG 106)	LEU345, VAL102, ARG106, TYR341, HIE75, SER339, ARG499, GLN178, ALA502, ILE503, LEU338, MET508, PHE504, VAL509, TRP373, ALA513, PHE567, GLY512, SER516, TYR371, LEU517, VAL335, LEU103, ILE331, MET99
VMSB8	-8. 193	Pi-Pi Stacking (TYR 341),	ALA502, ARG499, SER339, TYR341, ARG106, VAL102, LEU345, LEU517, LEU520, ALA513, VAL335, SER516, VAL509, GLY512, PHE367, TRP, 373, LEU370, MET508, TYR371, PHE504, LEU338, ILE503, GLN178, HIE75
VMSB3	-7 . 856	Pi-Pi Stacking (ARG 106)	ARG499, SER339, HIE75, VAL509, TYR341, ARG106, MET99, VAL102, LEU103, LEU517, LEU345, VAL335, ALA513, SER516, TYR371, GLY512, PHE367, TRP373, TYR334, LEU338, PHE504, ALA502, GLN178,ILE503
VMSB1	-7.826	Pi-Pi Stacking (ARG106), H-bond	MET99, ARG106, TYR34, VAL509, SER339, ARG499, HIS75, ALA502, ILE503, PHE504, GLN178, TYR334,

		(ARG499)	LEU338, GLY512, PHE367, TRP373, TYR371, SER516, VAL335, ALA513, LEU517, LEU345, LEU103, VAL102
VMSB10	-7 . 713	Pi-Pi Stacking (TYR 341), Pi-Pi Stacking (ARG 106)	PHE504, GLN178, VAL509, HIE75, SER339, ARG106, TYR341, LEU345, VAL102, LEU520, SER516, LEU517, VAL335, TYR334, ALA513, GLY512, TRP373, LEU370, MET508, TYR371, LEU338, ALA502, GLY505, ARG499, ILE503
VMSB13	-7 . 578	Pi-Pi Stacking (ARG 106)	ARG499, VAL509, HIE75, TYR341, SER339, ARG106, MET99, VAL102, LEU103, LEU334, LEU517, ALA513, VAL335, SER516, TYR371, GLY512, PHE367, TRP373, TYR334, LEU338, ALA502, PHE504, GLN178, ILE503
VMSB5	-7 . 405	Pi-Pi Stacking (TRP 373), Pi-cation (ARG 106)	GLY512, LEU370, SER516, TRP373, ALA513, VAL335, ARG106, LEU517, MET99, VAL102, TYR341, LEU345, SER339, LEU338, VAL509, HIE75, ILE503, ARG499, PHE504, ALA502, GLN 178, MET508, TYR371, PHE367
VMSB15	-5. 608	Pi-Pi Stacking (TYR 341)	ARG499, HIE75, SER339, TYR341, VAL102, ARG106, LEU517, LEU345, LEU520, VAL335, SER516, TYR334, ALA513, VAL509, GLY512, TRP373, LEU370, MET508, TYR371, LEU338, PHE504, ILE503, GLN178, ALA502

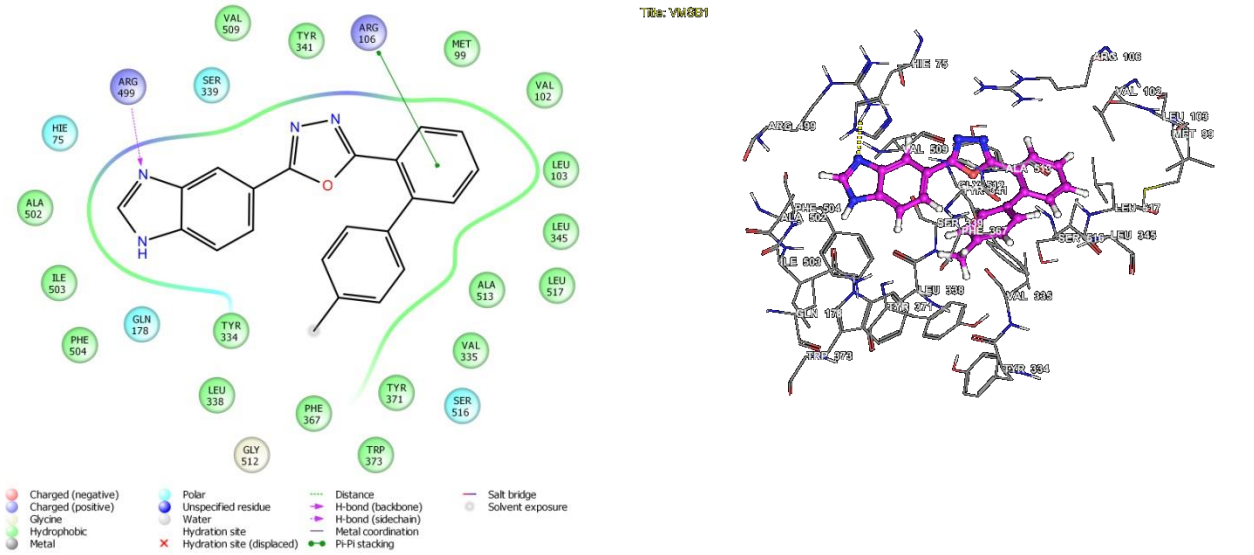

Figure (18): Docking process of VMSB1 a. 2D structure, b. 3D structure

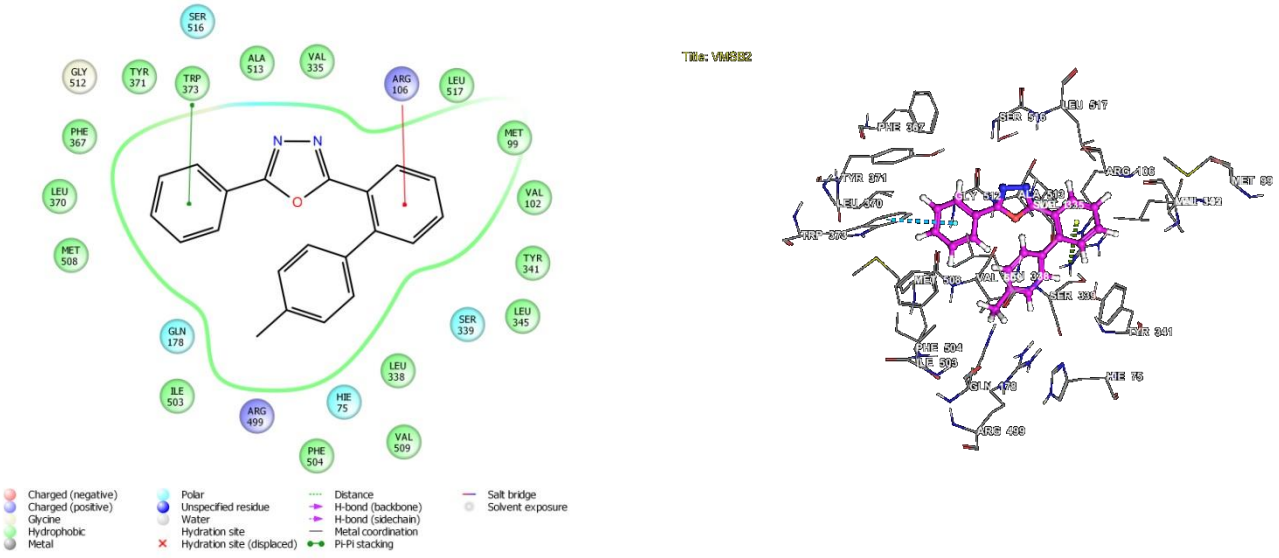

Figure (19): Docking process of VMSB2 a. 2D structure, b. 3D structure

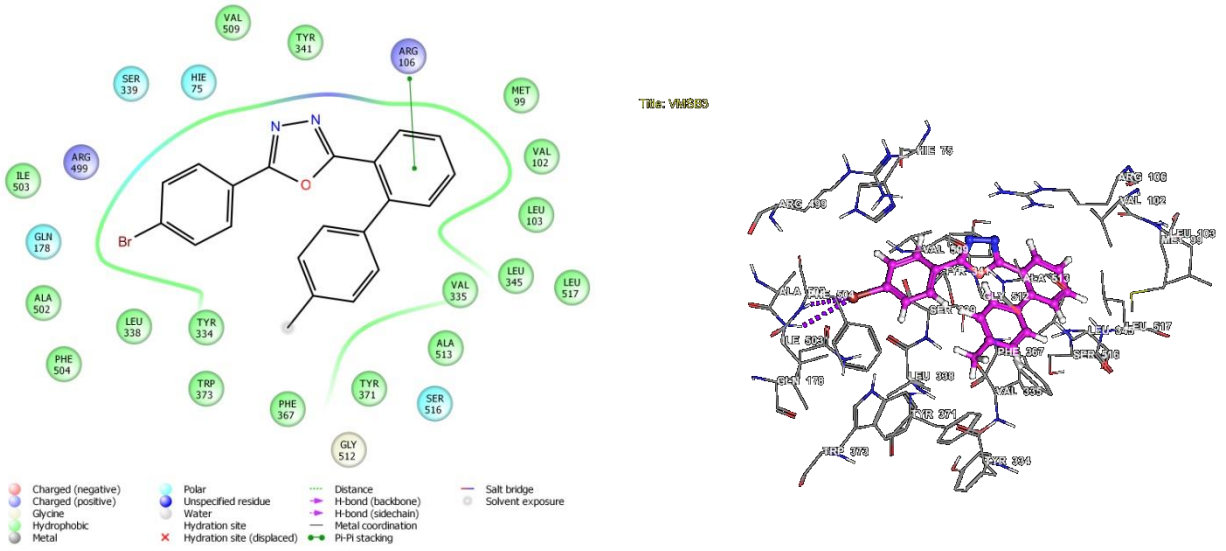

Figure (20): Docking process of VMSB3 a. 2D structure, b. 3D structure

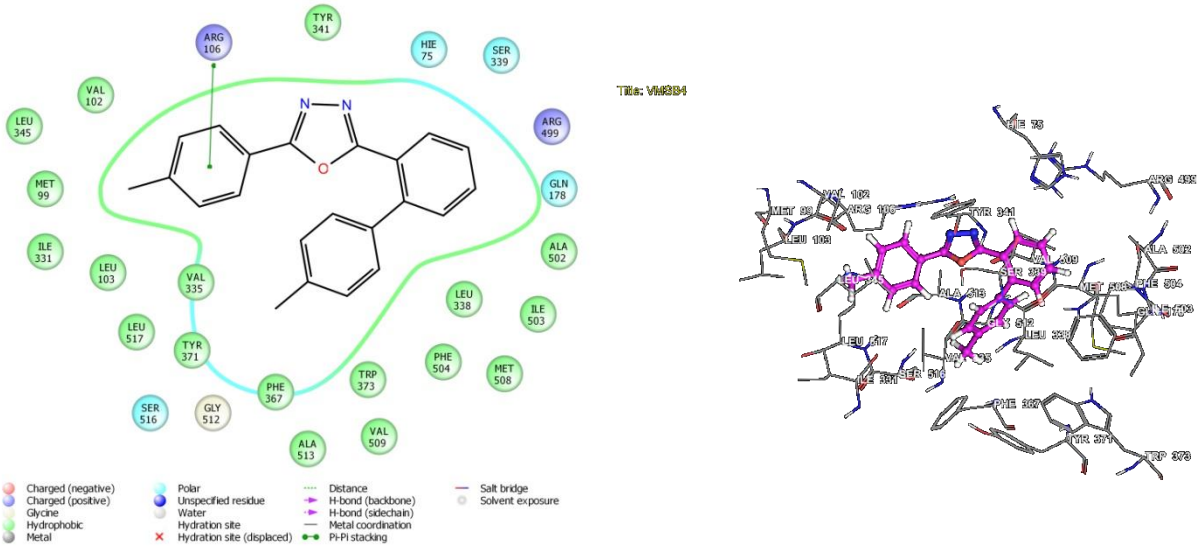

Figure (21): Docking process of VMSB4 a. 2D structure, b. 3D structure

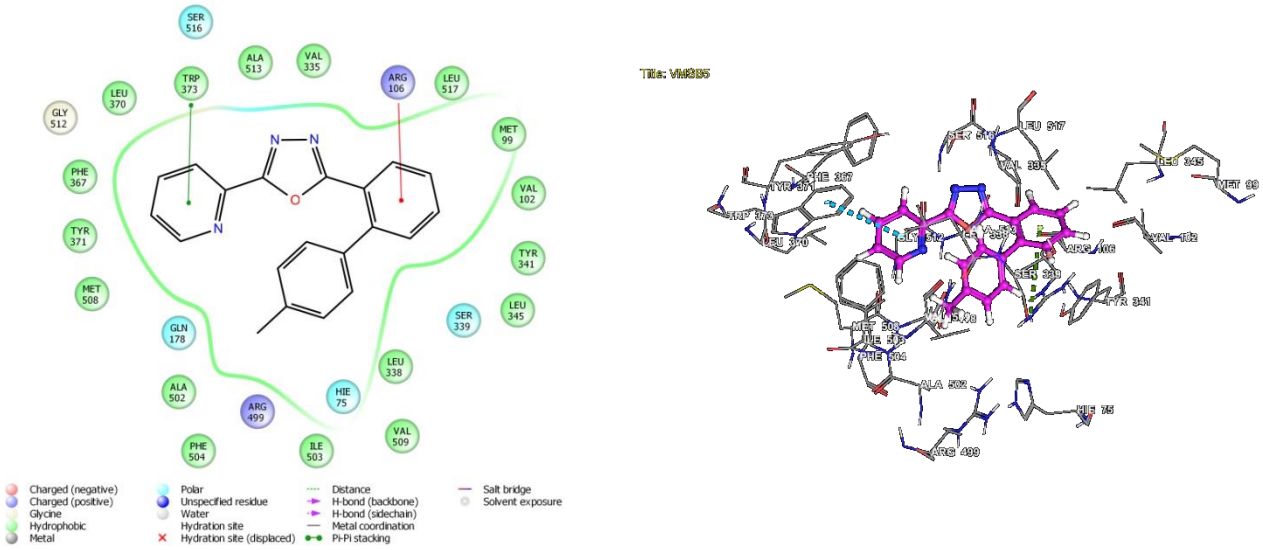

Figure (22): Docking process of VMSB5 a. 2D structure, b. 3D structure

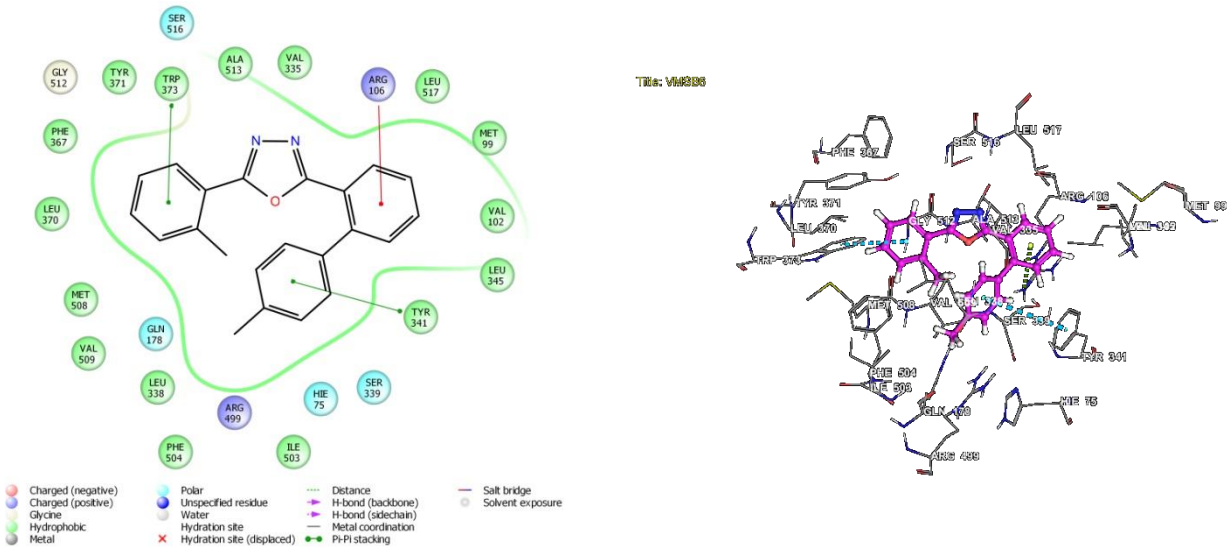

Figure (23): Docking process of VMSB6 a. 2D structure, b. 3D structure

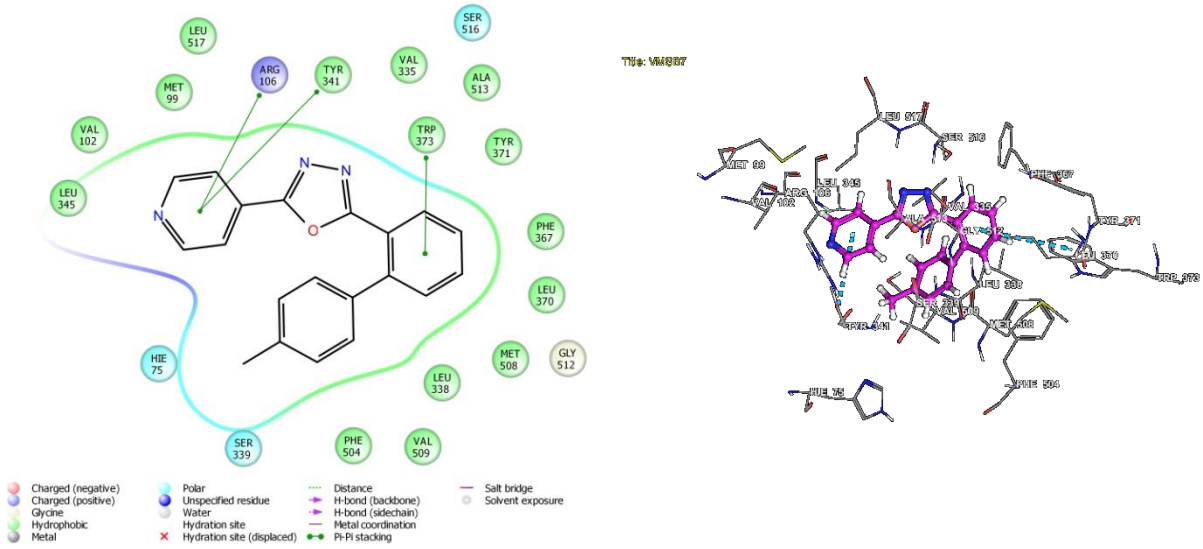

Figure (24): Docking process of VMSB7 a. 2D structure, b. 3D structure

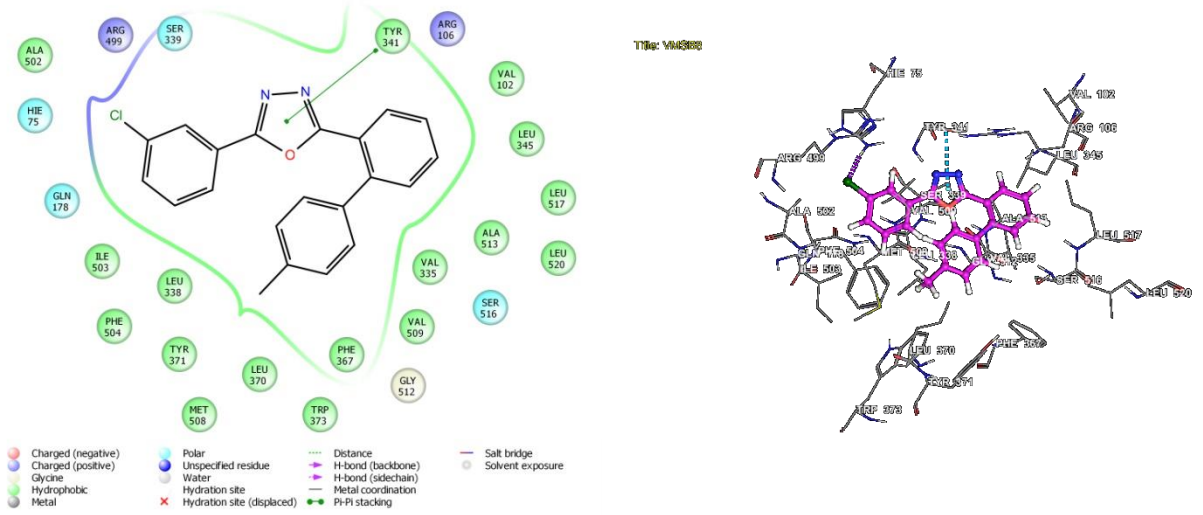

Figure (25): Docking process of VMSB8 a. 2D structure, b. 3D structure

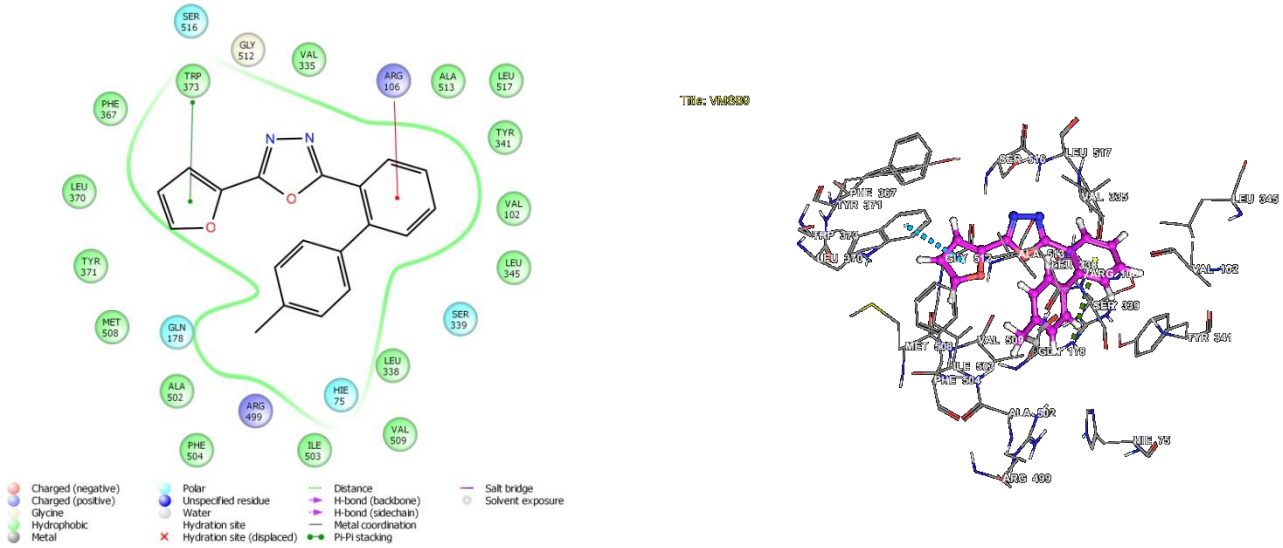

Figure (26): Docking process of VMSB9 a. 2D structure, b. 3D structure

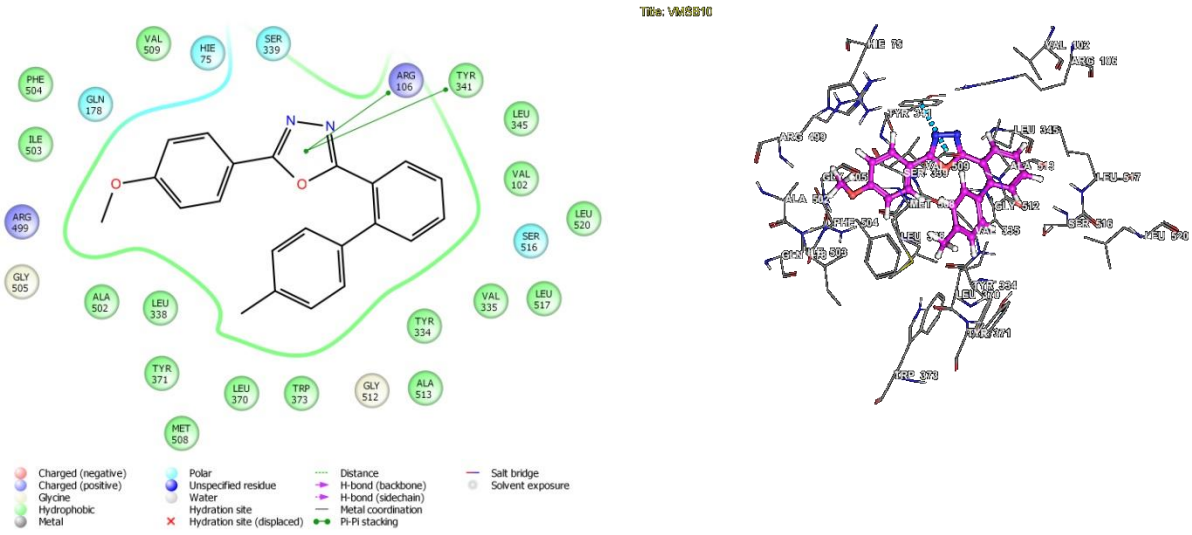

Figure (27): Docking process of VMSB10 a. 2D structure, b. 3D structure

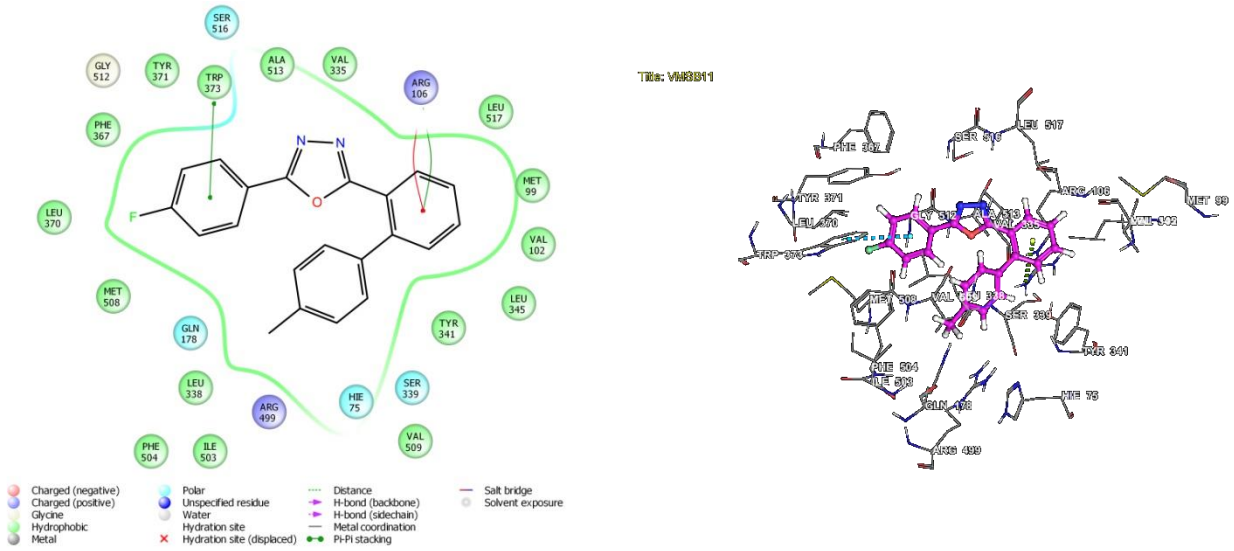

Figure (28): Docking process of VMSB11 a. 2D structure, b. 3D structure

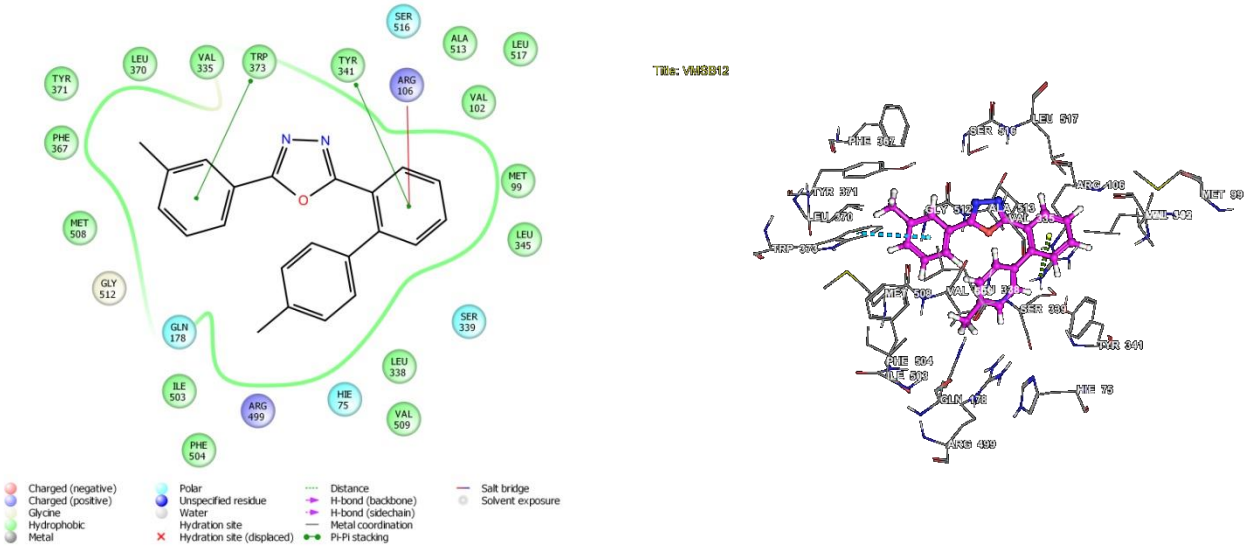

Figure (29): Docking process of VMSB12 a. 2D structure, b. 3D structure

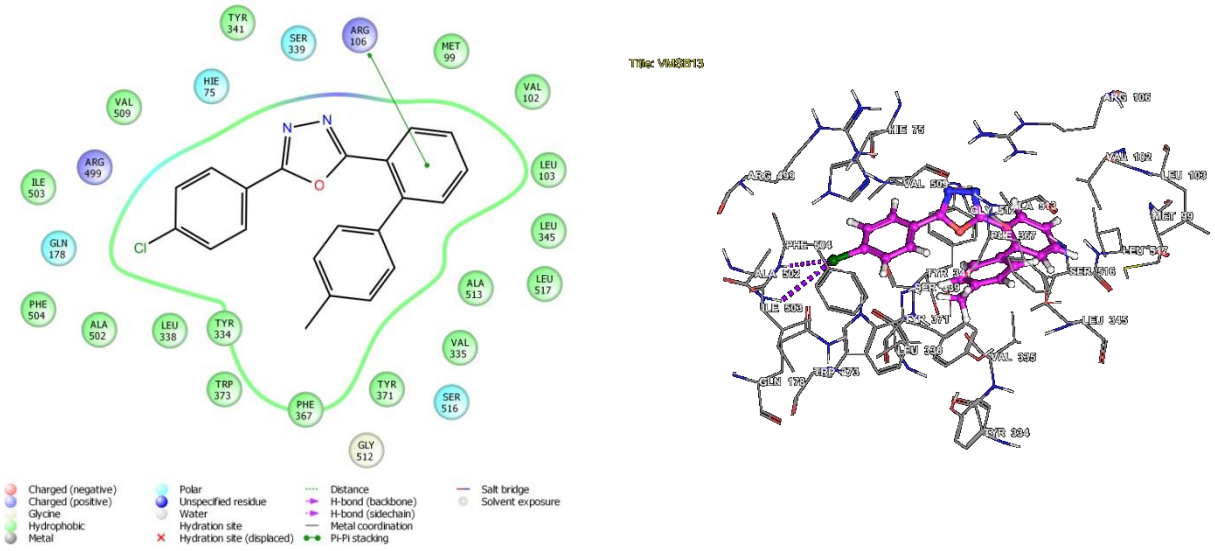

Figure (30): Docking process of VMSB13 a. 2D structure, b. 3D structure

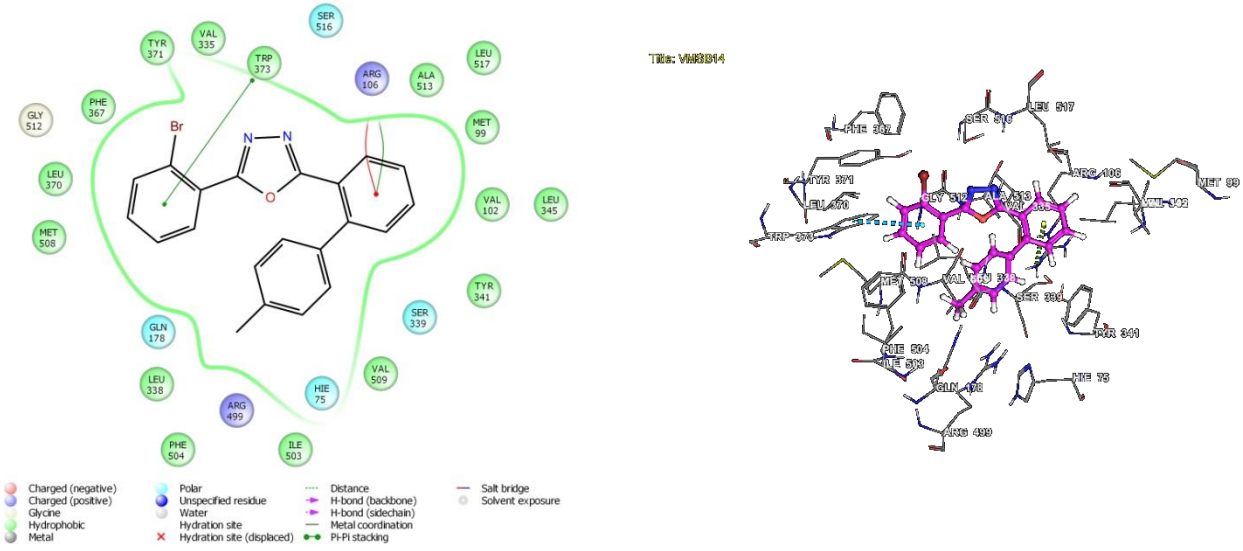

Figure (31): Docking process of VMSB14 a. 2D structure, b. 3D structure

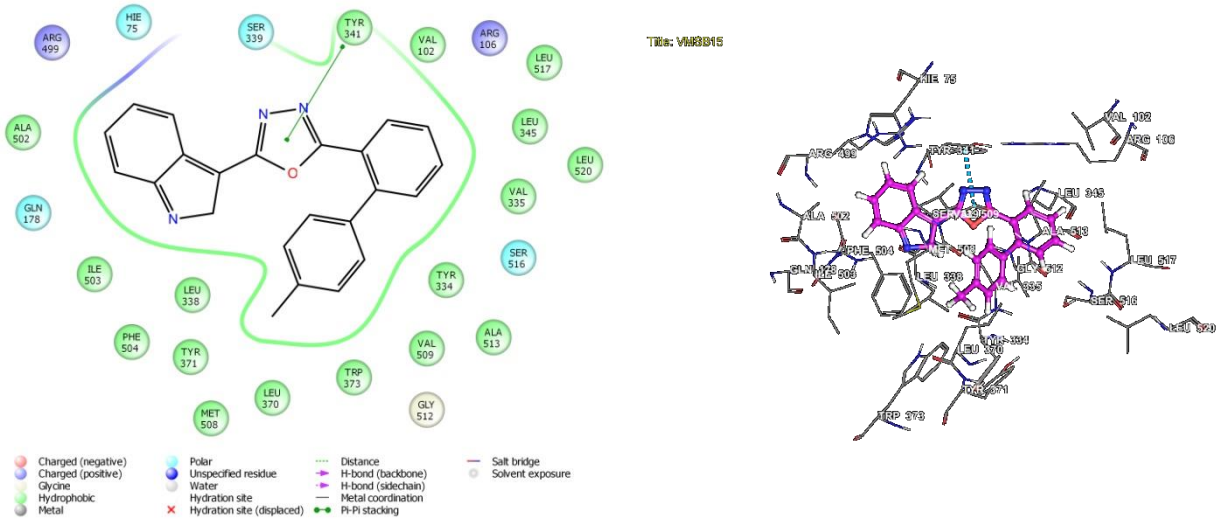

Figure (32): Docking process of VMSB15 a. 2D structure, b. 3D structure

CONCLUSION

In this research, a virtual docking process has been conducted using AutoDock software. The docking process was carried out among the VMSB-based compounds. Fifteen VMSB compounds were studied to find the best of them in terms of the linkage with the amino acid and consequently nominate the best inhibitor to the COX2 enzyme. The results have showed that the VMSB2 is the best compound among the fifteen compounds that has the top value of the docking score. It was concluded that the amino acid TRP373 is the suitable match for this compound.

References

1- Salum, L.; Polikarpov, I.; Andricopulo, A.D. Structure-based approach for the study of estrogen receptor binding affinity and subtype selectivity. *J. Chem. Inf. Model.* **2008**, *48*, 2243–2253.
2- Lipinski, C.A.; Lombardo, F.; Dominy, B.W.; Feeney, P.J. Experimental and computational approaches to estimate solubility and permeability in drug discovery and development settings. *Adv. Drug Deliv. Rev.* **2012**, *64*, 4–17.
3- Berman, H.M. The protein data bank. *Nucleic Acids Res.* **2000**, *28*, 235–242.
4- López-Vallejo, F.; Caulfield, T.; Martínez-Mayorga, K.; Giulianotti, M.A.; Houghten, R.A.; Nefzi, A.; Medina-Franco, J.L. Integrating virtual screening and combinatorial chemistry for accelerated drug discovery. *Comb. Chem. High Throughput Screen.* **2011**, *14*, 475–487.
5- Xuan-Yu Meng, Hong-Xing Zhang, Mihaly Mezei, and Meng Cui. Molecular Docking: A powerful approach for structure-based drug discovery. Curr Comput Aided Drug Des. **2011** June 1; 7(2): 146–157.
6- A.M. Vijesh , Arun M. Isloor , Sandeep Telkar , T. Arulmoli , Hoong-Kun Fun. Molecular docking studies of some new imidazole derivatives for antimicrobial properties. Arabian Journal of Chemistry **(2013)** 6, 197–204.
7- Huang, S.Y.; Zou, X. Advances and challenges in protein-ligand docking. Int. J. Mol. Sci. **2010**, 11, 3016–3034.
8- https://www.verywell.com/cyclooxygenase-cox-1-and-cox-2-2552188. Sited at 9/2/2017.
9- Kargman S, Charleson S, Cartwright M, Frank J, Mancini J, Evans J and O'Neill G. (1996). Gastroenterology, 111, 445 – 454.
10- Allison MC, Howatson AG, Torrance CJ, Lee FD and Russell RI. (1992). N. Engl. J. Med., 327, 749 – 754.
11- Hirst JJ, Teixeira FJ, Zakar T and Olson DM. (1995). J. Clin. Endocrinol. Metab., 80, 517 – 523.
12- Leonardo G. Ferreira , Ricardo N. dos Santos, Glaucius Oliva and Adriano D. Andricopulo. Molecular Docking and Structure-Based Drug Design Strategies. *Molecules* **2015**, *20*, 13384-13421.
13- Kalpesh patel, Ravi shah, **(2009)** *Perituma posthuma*, 1(3), 957.
14- O. P. Agarwal, **(2002)** *Organic chemistry reaction and reagents*, 826-828.
15- Ainsworth, **(1965)** *J. Am.Chem.Soc*., 87, 5800. (sited in www.shodhganga.inflibnet.ac.in, at 2/12/2016).
16- S. Rollas, **(2002)** *IL Farmaco*, 57, 171.(sited: www.shodhganga.inflibnet.ac.in, at 2/12/2016).
17- Arvind K. Singh,Vinay Kr.Sahu,Deepmala Yadav. Biological Activities of 2, 5-Disubstituted –1, 3, 4-Oxadiazoles. International Journal of Pharma Sciences and Research.Vol.2(6), **2011**,135-147.